PERGAMON

Scripta Materialia 47 (2002) 515–520

Scripta MATERIALIA

www.actamat-journals.com

Phase transformations in a Cu–14.2Al–12.0Ni alloy

C.H. Chen *, T.F. Liu

Department of Materials Science and Engineering, National Chiao Tung University, 300 Hsinchu, Taiwan, ROC

Received 6 February 2002; received in revised form 5 March 2002; accepted 28 May 2002

Abstract

The as-quenched microstructure of the Cu–14.2Al–12.0Ni alloy was $D0_3$ phase containing extremely fine L–J precipitates, where the $D0_3$ phase was formed by an A2 → B2 → $D0_3$ continuous ordering transition during quenching. Besides, the addition of nickel to the Cu–14.2Al binary alloy would raise the B2 → β transition temperature.

Keywords: Cu–Al–Ni alloy; Phase transformation; TEM; Ordering

1. Introduction

Phase transformations in Fe–Al and Fe–Al–Mn alloys have been extensively studied by many workers using transmission electron microscopy [1–6]. They have shown that if the $D0_3$ phase was formed by continuous ordering transition during quenching, it was occurred through an A2 (disordered body-centered cubic) → B2 → $D0_3$ transition. The A2 → B2 transition produced a/4⟨1 1 1⟩ anti-phase boundaries (APBs) and the B2 → $D0_3$ transition produced a/2⟨1 0 0⟩ APBs [3–7]. Similarly, several investigators proposed that in Cu–Al, Cu–Al–Mn and Cu–Al–Ni alloy systems, the $D0_3$ phase could also be formed by the A2 → B2 → $D0_3$ continuous ordering transition during quenching from the single β phase (A2) region [8–13]. However, in contrast to the above proposition, other workers claimed that the $D0_3$ phase was occurred through an A2 → $D0_3$ transition rather than the A2 → B2 → $D0_3$ transition [14–17]. The reason for the discrepancy between them is that, to date, the existence of the B2 phase-field was only determined by using X-ray diffraction method, thermomagnetic method, electrical resistometry and thermal analysis [8–13], no a/4⟨1 1 1⟩ APBs could be observed by transmission electron microscopy [8–17]. It means that no direct evidence confirmed the existence of the B2 phase-field in these alloy systems. Recently, we performed a transmission electron microscopy examination on the phase transformations of the Cu–14.2Al–12.0Ni alloy. Consequently, it was found that the a/4⟨1 1 1⟩ APBs indeed could be observed in the as-quenched alloy. Besides, the addition of nickel in the Cu–Al binary alloy would raise the B2 → β transition temperature.

2. Experimental procedure

The alloy, Cu–14.2wt.%Al–12.0wt.%Ni, was prepared in a vacuum induction furnace by using

* Corresponding author. Tel.: +886-3-712121x55365; fax: +886-3-5724727.

E-mail address: andychen.mse86g@nctu.edu.tw (C.H. Chen).

1359-6462/02/$ - see front matter
PII: S1359-6462(02)00192-6

99.9% copper, 99.9% aluminum and 99.9% nickel. The melt was chill cast into a $30 \times 50 \times 200$ mm copper mold. After being homogenized at 1050 °C for 72 h, the ingot was sectioned into 2.0 mm thick slices. These slices were subsequently solution heat-treated at 1050 °C for 1 h and then quenched into iced-brine. The aging processes were performed at temperatures ranging from 500 to 1000 °C for various times in a vacuum heat-treated furnace. Electron microscopy specimens were prepared by means of a double-jet electropolisher with an electrolyte of 70 pct methanol and 30 pct nitric acid. Electron microscopy was performed on a JEOL 2000FX scanning transmission electron microscope operating at 200 kV.

3. Results and discussion

Fig. 1(a) is a bright-field (BF) electron micrograph of the as-quenched alloy, clearly exhibiting the presence of the extremely fine precipitates with a mottled structure within the matrix. Fig. 1(b) and (c) show two selected-area diffraction patterns (SADPs) of the as-quenched alloy. It is seen in these SADPs that in addition to the reflection spots corresponding to the $D0_3$ phase [16–19], some extra spots with streaks can be observed. Compared to our previous studies in $Cu_{2.2}Mn_{0.8}Al$ and Cu–14.6Al–4.3Ni alloys [19,20], it is found that the extra spots with streaks are the same as those of the L–J phase with two variants. The L–J phase has an orthorhombic structure with lattice parameters $a = 0.413$ nm, $b = 0.254$ nm and $c = 0.728$ nm, which was firstly found and identified by the present workers in the $Cu_{2.2}Mn_{0.8}Al$ alloy [20]. Fig. 1(d) is a $(0\,0\,2)_{D0_3}$ dark-field (DF) electron micrograph of the same area as Fig. 1(a), revealing the presence of the small B2 domains with $a/4\langle 1\,1\,1\rangle$ APBs. Fig. 1(e), a $(\bar{1}\,1\,1)_{D0_3}$ DF electron micrograph, shows the presence of the extremely fine $D0_3$ domains with $a/2\langle 1\,0\,0\rangle$ APBs. Since the sizes of both B2 and $D0_3$ domains are very small, it is therefore deduced that the B2 and $D0_3$ domains were formed by the $\beta \rightarrow B2 \rightarrow D0_3$ continuous ordering transition during quenching [3–7]. Fig. 1(f) is a DF electron micrograph taken with the reflection spot marked as "1" in Fig. 1(b), clearly revealing the presence of the extremely fine L–J precipitates. On the basis of the above observations, it is concluded that the microstructure of the present alloy in the as-quenched condition is $D0_3$ phase containing extremely fine L–J precipitates, where the $D0_3$ phase was formed by the $\beta \rightarrow B2 \rightarrow D0_3$ continuous ordering transition during quenching.

Fig. 2(a) is a BF electron micrograph of the alloy aged at 700 °C for 1 h and then quenched. Fig. 2(b), a $(0\,0\,2)_{D0_3}$ DF electron micrograph of the same area as Fig. 2(a), shows that the B2 domains have well grown. Fig. 2(c) and (d) are $(\bar{1}\,1\,1)_{D0_3}$ and $(0\,\bar{2}\,0_1)_{L-J}$ DF electron micrographs, revealing the presence of the $D0_3$ domains and the L–J precipitates, respectively. It is obvious in Fig. 2(c) and (d) that the sizes of both the $D0_3$ domains and the L–J precipitates are very extremely fine. Therefore, it is reasonable to believe that these two phases were formed during quenching; otherwise, their sizes should be increased at the aging temperature [5,7]. This indicates that the microstructure of the alloy present at 700 °C is the single B2 phase. Transmission electron microscopy examinations of thin foils indicated that the single B2 phase could be preserved up to 975 °C. An example is shown in Fig. 3. It is seen in this figure that along with the growth of the B2 domains, the $a/4\langle 1\,1\,1\rangle$ APBs had gradually disappeared. In Fig. 3, it is also seen that the dark contrast is visible within the B2 domains because of the presence of the extremely fine L–J precipitates. Progressively higher temperature aging and quenching experiments indicated that when the alloy was aged at 1000 °C for 1 h and then quenched, only quenched-in B2 and $D0_3$ domains (the sizes being comparable to those observed in the as-quenched alloy) could be observed, as illustrated in Fig. 4. This indicates that the microstructure existing at 1000 °C or above is the single disordered β phase.

Based on the above observations, three important experimental results are discussed below. (I) In the previous studies [9–17], it is seen that no evidence of the $a/4\langle 1\,1\,1\rangle$ APBs could be detected by transmission electron microscopy. The reason for the absence of the $a/4\langle 1\,1\,1\rangle$ APBs was proposed that the $a/4\langle 1\,1\,1\rangle$ APB energy in the Cu–Al–Ni and Cu–Al–Mn alloys is very high,

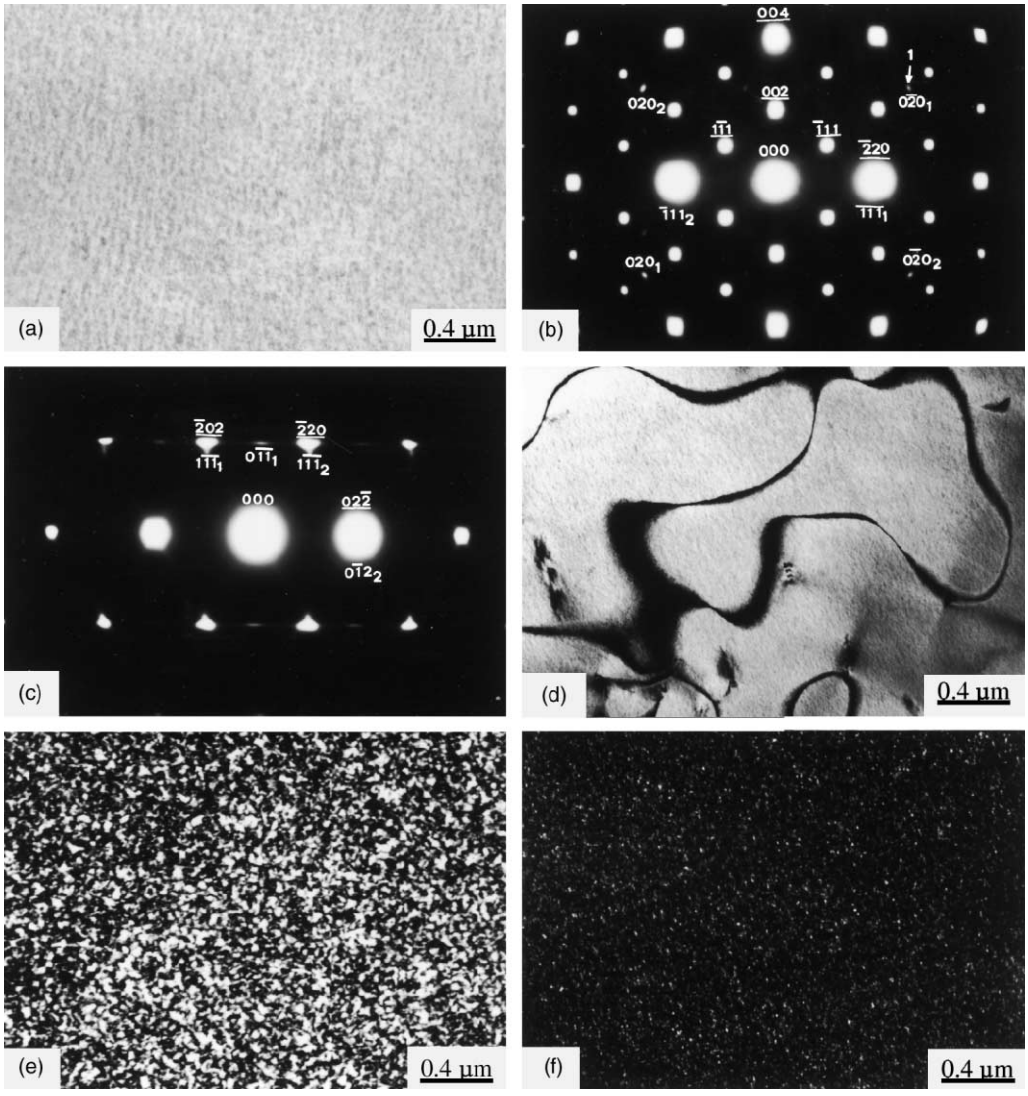

Fig. 1. Electron micrographs of the as-quenched alloy. (a) BF, (b) and (c) two SADPs. The zone axes of the $D0_3$ phase are (b) [1 1 0] and (c) [1 1 1], respectively ($\underline{hkl}$ = $D0_3$ phase, hkl_{1or2} = L–J phase, 1: variant 1; 2: variant 2). (d) and (e) $(0\,0\,2)_{D0_3}$ and $(\bar{1}\,1\,1)_{D0_3}$ DF, respectively. (f) DF micrograph, which was taken with the reflection spot marked as 1 in (b).

therefore, the B2 domains would grow to reach the whole grains during quenching [9,13]. However, the $a/4\langle 1\,1\,1\rangle$ APBs indeed could be observed in the present alloy. In addition to contain higher nickel content, the chemical composition of the present alloy is similar to that examined by other workers in the Cu–Al–Ni alloys [16,17]. It seems to imply that the increase of the nickel content could decrease the $a/4\langle 1\,1\,1\rangle$ APB energy significantly. Therefore, the $a/4\langle 1\,1\,1\rangle$ APBs became visible, as observed in Fig. 1(d). (II) To date, no information concerning the B2 $\rightarrow$ β transition temperature of the Cu–Al–Ni ternary alloys has been provided in the literatures. However, it is seen in the Cu–Al binary alloy phase diagram that the B2 $\rightarrow$ β transition temperature of the Cu–14.2Al binary

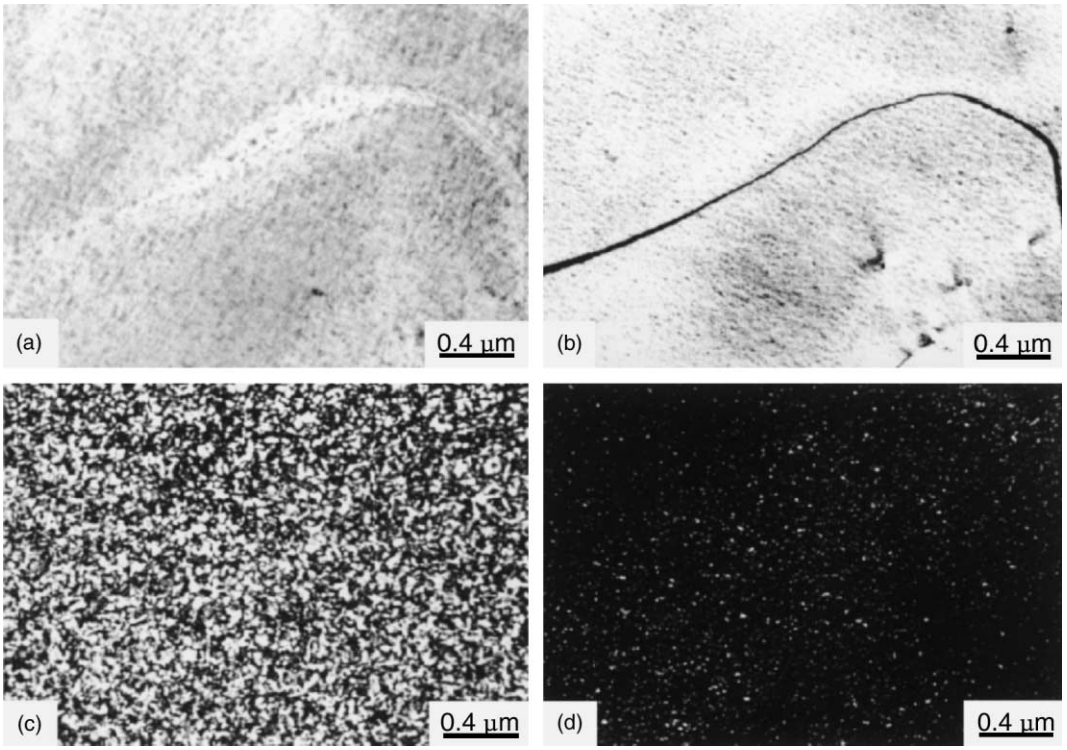

Fig. 2. Electron micrographs of the alloy aged at 700 °C for 1 h. (a) BF, (b) and (c) $(0\,0\,2)_{D0_3}$ and $(\bar{1}\,1\,1)_{D0_3}$ DF, respectively. (d) $(0\bar{2}0_1)_{L-J}$ DF.

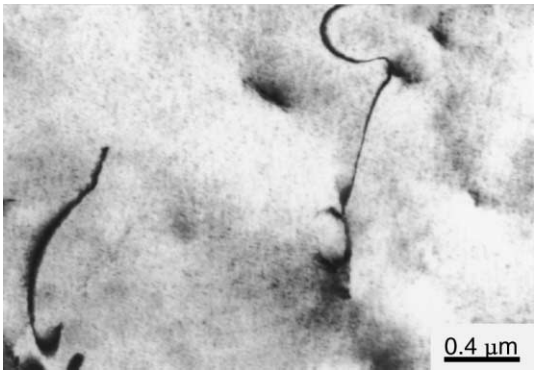

Fig. 3. $(0\,0\,2)_{D0_3}$ DF electron micrograph of the alloy aged at 975 °C for 20 min.

alloy was about 710 °C [10,11]. In the present alloy, this transition temperature was found to be raised to somewhere between 975 and 1000 °C. This indicates that the B2 → β transition temperature would be increased because of the nickel addition. This feature is similar to that observed by the present workers in an Fe–23.2Al–4.1Ni alloy [21]. In the previous study, we have shown that the addition of nickel to the Fe–Al alloy could remarkably raise the B2 → β transition temperature. (III) It is worthwhile to mention that in the present study, an attempt to determine the B2 → $D0_3$ transition temperature was also made. Unfortunately, it was not successful. The reason for this is that when the present alloy was aged at 650 °C or below, other phases would occur rapidly to occupy the whole grains before the growth of the B2 or $D0_3$ domains. A typical example is shown in Fig. 5(a), which is a BF electron micrograph of the present alloy aged at 500 °C for 3 min and then quenched. Fig. 5(b) and (c), two SADPs, indicate that the microstructure present in Fig. 5(a) is a mixture of B2 phase and γ_1' martensite with internal twins [16], and the orientation relationship between the B2 phase and the

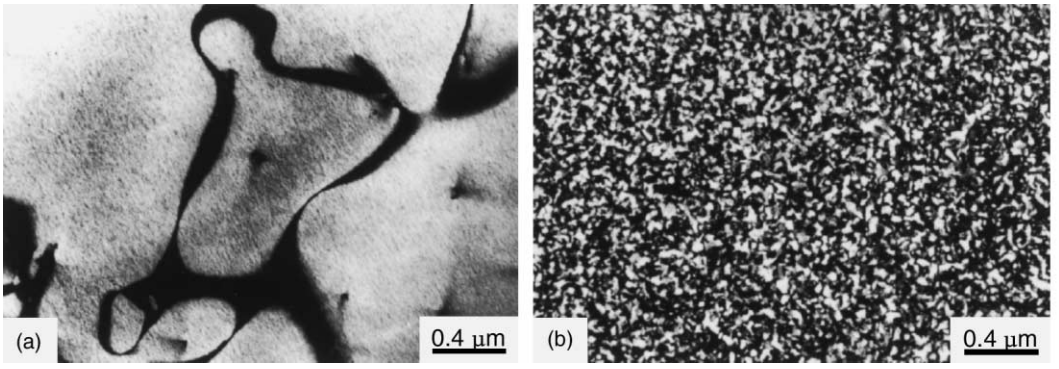

Fig. 4. (a) $(002)_{D0_3}$ and (b) $(\bar{1}11)_{D0_3}$ DF electron micrographs of the alloy aged at 1000 °C for 1 h.

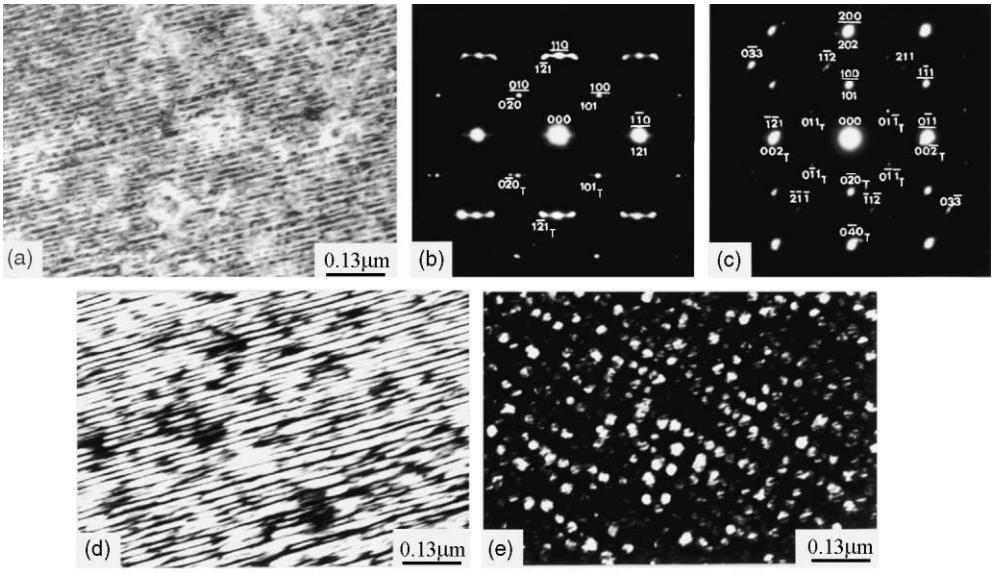

Fig. 5. Electron micrographs of the alloy aged at 500 °C for 3 min. (a) BF, (b) and (c) two SADPs. The zone axes of B2 phase, γ_1' martensite and internal twin are (b) [0 0 1], $[1\,0\,\bar{1}]$ and $[\bar{1}\,0\,1]$, (c) [0 1 1], $[1\,\bar{1}\,\bar{1}]$ and $[\bar{1}\,0\,0]$, respectively. (hkl = B2 phase, hkl = γ_1' martensite, hkl_T = internal twin.) (d) and (e) $(1\,\bar{2}\,1)_{\gamma_1'}$ and $(1\,0\,0)_{B2}$ DF.

γ_1' martensite is $[0\,0\,1]_{B2}//[1\,0\,\bar{1}]_{\gamma_1'}$ and $(1\,\bar{1}\,0)_{B2}//(1\,2\,1)_{\gamma_1'}$. The γ_1' martensite has an orthorhombic structure with lattice parameters $a = 0.4382$ nm, $b = 0.5356$ nm and $c = 0.4222$ nm [22]. Fig. 5(d) and (e) show the $(1\,\bar{2}\,1)_{\gamma_1'}$ and $(1\,0\,0)_{B2}$ DF electron micrographs of the same area as Fig. 5(a), revealing the presence of the γ_1' martensite and B2 precipitates, respectively.

Finally, it is noted here that γ_2 precipitates were always reported to be observed in the Cu–(9.2–15.1)wt.%Al–(0–4.3)wt.%Ni alloys after being aged at temperatures ranging from 200 to 700 °C for various times [13–17,23]. However, in the present study, no evidence of the γ_2 precipitates could be detected. Therefore, it is reasonable to believe that the higher nickel addition in the Cu–Al–Ni

alloy would unfavor the precipitation of the γ_2 phase.

4. Conclusions

(1) The as-quenched microstructure of the Cu–14.2Al–12.0Ni alloy was $D0_3$ phase containing extremely fine L–J precipitates. In the as-quenched alloy, both the small B2 domains with $a/4\langle 1\,1\,1\rangle$ APBs and the extremely fine $D0_3$ domains with $a/2\langle 1\,0\,0\rangle$ APBs could be observed. This result strongly confirmed that the $D0_3$ phase was formed by the $A2 \rightarrow B2 \rightarrow D0_3$ continuous ordering transition during quenching.
(2) The addition of nickel to the Cu–14.2Al binary alloy would raise the $B2 \rightarrow \beta$ transition temperature.
(3) The higher nickel addition in the Cu–Al–Ni alloy would unfavor the precipitation of the γ_2 phase.

Acknowledgements

The author is pleased to acknowledge the financial support of this research by the National Science Council, Republic of China under Grant NSC90-2216-E-009-044. He is also grateful to M.H. Lin for typing.

References

[1] Liu TF, Uen GC, Chao CY, Lin YL, Wu CC. Metall Trans A 1991;22A:1407.
[2] Wu CC, Chou JS, Liu TF. Metall Trans A 1991;22A:2265.
[3] Lee JW, Liu TF. Mater Chem Phys 2001;69:192.
[4] Swann PR, Duff WR, Fisher RM. Metall Trans 1972;3:409.
[5] Allen SM, Cahn JW. Acta Metall 1976;24:425.
[6] Allen SM. Philos Mag 1977;36(1):181.
[7] Ikeda O, Himuro Y, Ohnuma I, Kainuma R, Ishida K. J Alloys Comp 1998;268:130.
[8] Soltys J, Stefaniak M, Holender J. Philos Mag B 1984;49(2):151.
[9] Nesterenko YG, Osipenko IA, Firstov SA. Fiz Metal Metalloved 1969;27(1):135.
[10] Liu XJ, Ohnuma I, Kainuma R, Ishida K. J Alloys Comp 1998;264:201.
[11] Kainuma R, Satoh N, Liu XJ, Ohnuma I, Ishida K. J Alloys Comp 1998;266:191.
[12] Bouchard M, Thomas G. Acta Metall 1975;23:1485.
[13] Zárubová N, Gemperle A, Novák V. Mater Sci Eng A 1997;A222:166.
[14] Dvorack MA, Kuwano N, Polat S, Chen H, Wayman CM. Scripta Metall 1983;17:1333.
[15] Thomas DL. J Inst Metals 1966;94:250.
[16] Kuwano N, Wayman CM. Metall Trans A 1984;15A:621.
[17] Singh J, Chen H, Wayman CM. Metall Trans A 1986;17A:65.
[18] Liu TF, Chou JS, Wu CC. Metall Trans A 1990;21A:1891.
[19] Tan J, Liu TF. Mater Chem Phys 2001;70:49.
[20] Jeng SC, Liu TF. Metall Trans A 1995;26A:1353.
[21] Liu TF, Jeng SC, Wu CC. Metall Trans A 1992;23A:1395.
[22] Otsuka K, Sakamoto H, Shimizu K. Trans JIM 1979;20:244.
[23] Sun YS, Lorimer GW, Ridley N. Metall Trans A 1990;21A:575.